Peer-reviewed version available at *J. Clin. Med.* **2019**, *8*, 1374; doi:10.3390/jcm8091374

Article

ADCK2 haploinsufficiency reduces mitochondrial lipid oxidation and causes myopathy associated with CoQ deficiency

Luis Vázquez-Fonseca[1,9§], Jochen Schäfer[2,§], Ignacio Navas-Enamorado[1,7], Carlos Santos-Ocaña[1,10], Juan D. Hernández-Camacho[1,10], Ignacio Guerra[1], María V. Cascajo[1,10], Ana Sánchez-Cuesta[1,10], Zoltan Horvath[2#], Emilio Siendones[1], Cristina Jou[3,10], Mercedes Casado[3,10], Purificación Gutiérrez[1], Gloria Brea-Calvo[1,10], Guillermo López-Lluch[1,10], Daniel J. M. Fernández-Ayala[1,10], Ana B. Cortés-Rodríguez[1,10], Juan C. Rodríguez-Aguilera[1,10], Cristiane Matté[4], Antonia Ribes[5,10], Sandra Y. Prieto-Soler[6], Eduardo Dominguez-del-Toro[6], Andrea di Francesco[8], Miguel A. Aon[8], Michel Bernier[8], Leonardo Salviati[9], Rafael Artuch[3,10], Rafael de Cabo[8], Sandra Jackson[2] and Plácido Navas[1,10,*]

[1] [1]Centro Andaluz de Biología del Desarrollo, Universidad Pablo de Olavide-CSIC-JA, Sevilla 41013, Spain
[2]Department of Neurology, Carl Gustav Carus University Dresden, 01307 Dresden, Germany. [#] Present address: Department of Neurology, University of Szeged, Szeged, Hungary.
[3]Clinical Chemistry and Pathology Departments, Institut de Recerca Sant Joan de Déu, Barcelona, Spain
[4]Departamento de Bioquímica, Instituto de Ciências Básicas da Saúde, Universidade Federal do Rio Grande do Sul. CEP 90035-003, Porto Alegre, RS, Brazil.
[5]Secciód'ErrorsCongènits del Metabolisme-IBC, Servei de Bioquímica I Genètica Molecular, Hospital Clinic, Barcelona, Spain
[6]División de Neurociencias, Universidad Pablo de Olavide, Sevilla 41013, Spain
[7]Boston University School of Medicine, Boston, Massachusetts, USA
[8]Translational Gerontology Branch, National Institute on Aging, National Institutes of Health, 251 Bayview Boulevard, Suite 100, Baltimore, Maryland, USA
[9]Clinical Genetics Unit, Department of Women and Children's Health, University of Padova, and IRP Città della Speranza, Padova, Italy
[10]CIBERER, Instituto de Salud Carlos III, Madrid, Spain
[§]These authors have equally contributed to this work.
* Correspondence: pnavas@upo.es

Abstract: Fatty acids and glucose are the main bioenergetic substrates in mammals that are alternatively used during the transition between fasting and feeding. Impairment of mitochondrial fatty acid oxidation causes mitochondrial myopathy leading to decreased physical performance. Here, we report that haploinsufficiency of ADCK2, a member of the aarF domain-containing mitochondrial protein kinase family, in human is associated with liver dysfunction and severe mitochondrial myopathy with lipid droplets in skeletal muscle. In order to better understand the etiology of this rare disorder, we generated a heterozygous *Adck2* knockout mouse model to perform in vivo and cellular studies using integrated analysis of physiological and omics data (transcriptomics-metabolomics). The data show that *Aldh2*+/- mice exhibits impaired fatty acid oxidation, liver dysfunction, and mitochondrial myopathy in skeletal muscle resulting in lower physical performance. Significant decrease in CoQ biosynthesis was observed and supplementation with CoQ partially rescued the phenotype both in the human subject and mouse model. These results indicate that ADCK2 is involved in organismal fatty acid metabolism and in CoQ biosynthesis in skeletal muscle. We propose that patients with isolated myopathies and myopathies involving lipid accumulation be tested for possible *ADCK2* defect as they are likely to be responsive to CoQ supplementation.

Keywords: Coenzyme Q deficiency; mitochondrial disease; respiratory chain; fatty acids; myopathy; *ADCK2*

1. Introduction

The liver, adipose tissue, and skeletal muscle regulate systemic metabolic flexibility in order to maintain energy homeostasis during the fast-fed transition [1]. The ability to switch between glucose and fatty acid (FA) catabolism defines metabolic flexibility in times of energy abundance (e.g., feeding) and restriction. [2]. Mitochondria play a central role in cellular energy metabolism by providing reducing equivalents from the tricarboxylic acid cycle and FA -oxidation to the respiratory chain (MRC), which is responsible for matching energy supply with demand. Coenzyme Q (CoQ) is a fat-soluble compound that transfers electrons between complex I and II to complex III of the MRC, and also receives electrons from dihydroorotate dehydrogenase and sulfide:quinone oxidoreductase [3]. Mitochondria are the site for substrate selection, namely glucose or fatty acids, depending upon energy demand [4] and CoQ contributes to determine the source of electrons for (?) complex I (NADH) vs. complex II ($FADH_2$) [5].

Defects in the mitochondrial -oxidation pathway elicit clinically heterogeneous myopathies such as multiple acyl-CoA dehydrogenase deficiency (MADD), an autosomal recessive disorder caused by mutations in *ETFDH*, a gene encoding electron-transfer flavoprotein:ubiquinone oxidoreductase, or in *ETFA* or *ETFB*, which encodes the alpha or beta subunit of electron transfer flavoprotein (ETF) [6,7]. Deficiency in ETF or ETFDH leads to impaired fatty acid oxidation and elevated levels of acyl-carnitines in plasma. The myopathic form of CoQ deficiency in some patients has been linked to a defect in fatty acid oxidation in skeletal muscle [8-10]. Moreover, impaired lipid metabolism associated with aberrant mitochondrial morphology have been found in response to the loss of mitofusin 2 (Mfn2), resulting in MRC defects due to a secondary deficiency in CoQ [11]. Mitochondrial diseases associated with CoQ deficiency are rare, and exhibit clinically heterogeneity that can be caused by mutations in *COQ* genes or genes encoded by either nuclear DNA or mitochondrial DNA [12-15].

The *ADCK* genes encode the aarF domain-containing mitochondrial protein kinases. Both human *ADCK3* (*COQ8A*) and *ADCK4* (*COQ8B*) show high homology to yeast *coq8* and can rescue the growth of *Δcoq8* yeast strain [16,17] by contributing to the stabilization of the CoQ biosynthesis complex [18]. ADCK3 has an unorthodox kinase function by harboring an ATPase activity [19]. Mutations in *ADCK3* cause autosomal recessive cerebellar ataxia with CoQ deficiency [18,20-26] whereas mutations in *ADCK4* promote CoQ-responsive steroid-resistant nephrotic syndrome through CoQ deficiency [27]. Silencing of *ADCK1* affects epithelial cell migration [28] while *ADCK2* silencing reduces the viability of glioblastoma-derived cancer cells [29] and estrogen receptor-positive breast tumors [30]. The depletion in *ADCK2* also significantly decreases the effect of TNFα on HIF-1α stability in osteosarcoma and prostate cancer cell lines [31]. However, no information is available about the role of ADCK2 in CoQ biosynthesis and, so far, there is no disease associated to this gene [13,32,33]

Here, we report that *Adck2* haploinsufficiency in mice causes mitochondrial dysfunction that affects mainly the skeletal muscle with evidence of liver steatosis without cognitive deficits or impairment in brain function. Mitochondrial myopathy associated with CoQ deficiency in skeletal muscle was observed along with marked perturbation in whole animal mitochondrial β-oxidation. This phenotype is reminiscent of that seen in a male patient with *ADCK2* haploinsufficiency that was partially rescued by CoQ supplementation. Our results show that *ADCK2* exerts a unique role in lipid homeostasis through control of the mitochondrial CoQ pool in muscle and organismal FA oxidation.

2. Materials and Methods

2.1. Mouse model

The *Adck2* knockout mouse model was produced at the Transgenic Animal Model Core, Biomedical Research Core Facilities of University of Michigan. All experiments were carried out in male mice from 3-12 months of age. Chimeras were produced by microinjecting C57BL/6-derived mutant ES cells into albino C57BL/6 host blastocysts obtained from the mating of C57BL/6-BrdCrHsd-Tyrc females with C57BL/6-BrdCrHsd-Tyrc males at the Transgenic Animal Model Core, Biomedical Research Core Facilities, University of Michigan. Any white pups from chimera breeding have contribution from both the ES cells and the host embryos and were labeled as C57BL/6-BrdCrHsd. The ES cell clones Adck2 ACB, Adck2 AB3, Adck2 AG2 were obtained from KOMP repository, Mouse Biology Program, University of California (www.komp.org). These cells are heterozygous for the *Adck2* deletion, and the host blastocysts are wild-type (WT) for the introduced mutation. The breeding of chimeric males with albino C57BL/6 females has produced black pups, which were derived from the ES cells. Because the ES cells are heterozygous for the mutation, half of the black pups were expected to be positive for the mutation. Mice were supplemented with 15 mg/kg/day of CoQ_{10} (Kaneka QH stabilized powder type P30) (Kaneka Pharma Europe, Brussels, Belgium) dissolved daily in the drinking water when indicated.

2.2. Cell strains and culture

Dermal fibroblasts from the study participant (subject II-3) and his sister (subject II-2), primary human fibroblasts MRC-5 (CCL-171, ATCC, Manassas, USA), and neonatal human dermal fibroblasts (HDFs) (PCS-210-010 and PCS-210-012, ATCC) were plated in separate six-well plates (40,000 cells/well) and cultured using Dulbecco's modified essential medium (DMEM) with 20% fetal calf serum (FCS). MEF preparations from WT, *Adck2*+/- and *Adck2*-/- mice were obtained from fetuses at day 9 postcoitum. As described elsewhere [34].

2.3. Targeted gene sequencing

Total DNA preparation was carried out following standard procedures. The mitochondrial and the exons and intron-exon boundaries of *ETFA, ETFB, ETFDH, ADCK1, ADCK3, ADCK4, ADCK5, PDSS1, PDSS2, COQ2, COQ3, COQ4, COQ5, COQ6, COQ7, COQ8A, COQ8B, COQ9, COQ10A, COQ10B* and *PPTC7* was were analyzed by Sanger sequencing. For quantification of the *ADCK2* or *adck2* transcript, RNA was extracted with easy-BLUE Total RNA extraction kit (iNtRON Biotechnology) according to manufacturer's instructions. One microgram of total RNA was used to obtain cDNA of human *ADCK2* gene with the iScript cDNA Synthesis Kit (Bio-Rad) following manufacturer's instructions. For sequencing of *ADCK2* mRNA from the index patient and other family members, RNA was isolated from cultured fibroblasts (RNeasy Plus Mini Kit -Qiagen) or from whole blood (PAXgene Blood RNA kit, PreAnalytiX), and reverse transcription was performed using the Quantitect Reverse Transcription kit (Qiagen). The entire *ADCK2* mRNA was amplified using 4 primer pairs with one primer from each pair spanning adjacent exons (http://www.autoprime.de/AutoPrimeWeb), and the amplicon was sequenced in the forward and reverse direction.

2.4. Measurement of plasma acyl-carnitine and urinary organic acids

Analysis of plasma acyl-carnitines in the index patient and other family members was performed on dry blood spots (Screening Labor, Hannover, Germany). For the animal studies, analysis of acyl-carnitines in plasma was performed by high-performance liquid chromatography, electrospray ionization and tandem mass spectrometry, in the underivatized form using a commercial kit of deuterated acylcarnitines (Perkin Elmer, Barcelona, Spain). The trimethylsilylated derivatives of organic acids were determined in mouse urine by gas chromatography/mass spectrometry (5975C Agilent Technologies). The signals (*m/z*) of the specific ions for every compound were corrected by the amount of the internal standard (undecanodioic; ion 345). For all urine samples, the same amount of creatinine was loaded onto the gas chromatograph/mass spectrometer. Plasma lactate levels were

Peer-reviewed version available at J. Clin. Med. 2019, 8, 1374; doi:10.3390/jcm8091374

measured with colorimetric lactate oxidase-peroxidase assay kit (Spinreact, Spain) as indicated by the manufacturer.

2.5. Yeast functional complementation

Yeast *YPL109c* mutants were transformed with the pYES2 vector containing the different versions of human *ADCK2*, and either the WT, site-directed mutant yeast *YPL109c*, or the empty vector for complementation experiments. Growth rate in non-fermentable carbon source (YPG medium) was determined as a marker of functional complementation.

2.6. Physical and behavioral tests

The rotarod performance test was performed to assess motor activity and coordination in mice. Animals were placed on an accelerating rotating rod (45 rpm max), and the time it took the mice to fall off of the rod was recorded. In the treadmill exhaustion test, the mice are forced to run on a treadmill (Treadmill Columbus 1055M-E50; Cibertec SA) at 8% inclination until exhaustion, starting at 10 m/min and increasing the speed by 5 m/min every 5 min until reaching 25 m/min. Exhaustion is achieved when animals who quit running refuse to move back to the treadmill 5 sec after receiving an electric foot shock [35]. Mouse muscle force was measured *in vivo* using a Grip Strength Columbus apparatus (Cibertec SA) as indicated [36]. Behavior was analyzed by passive avoidance to test associative memory and other tasks such as hot-plate sensitivity, exploratory locomotor activity by the open field actimeter [37], and associative short- and long-term memories were determined by novel object recognition (NOR) task as described [38]. (n=10 per group).

2.7. CoQ determination and biosynthesis

CoQ concentrations and biosynthesis rate were determined as described by Rodríguez-Aguilera et al. [39]. Moreover, CoQ biosynthesis rate was also determined by the incubation of cells with [^{3}H]-mevalonate, allowing also the analysis of cholesterol biosynthesis as described [40]. Specific activities were expressed as DPM.min^{-1}.mg protein^{-1}. Stable expression of *ADCK2* in human fibroblasts was achieved by the infection with lentiviral particles. The wild-type allele of human *ADCK2* was cloned in the pRRL.sin.EF1a-PGK-GFP plasmid to obtain the II-3-pRRL-ADCK2 plasmid needed for the production of lentiviral particles. 293T cells (5 x 10^6 cells per plate) were transfected with the II-3-pRRL-*ADCK2* plasmid, along with the packing plasmid psPAX2 and the capsid plasmid pMD2.G. After 16 h of incubation, the culture medium was replaced with fresh medium, which was collected 48 h later and subjected to filtration and centrifugation (26000 rpm, 2 h, 4ºC) in order to recover lentiviral particles. Human fibroblasts were seeded at 50,000 cells per well and expanded until reaching ~90% confluency, after which medium was changed and lentiviral particles (400 µL per well) were added. Twenty-four h later, more than 98% GFP-positive cells (a direct measure of transfection) were collected by cell sorting.

2.8. Mitochondrial biochemistry

Activities of NADH: coenzyme Q_1 oxidoreductase (complex I), succinate dehydrogenase (complex II), ubiquinol: cytochrome c oxidoreductase (complex III), NADH: cytochrome c reductase (complex I–III), succinate: cytochrome c reductase (complex II–III), cytochrome c oxidase (complex IV), and citrate synthase (CS) were determined in muscle biopsy from patients, in mouse skeletal muscle, and in fibroblast lysates by spectrophotometric assays as described [41]. Oxygen Consumption Rate (OCR) based on glucose as energy substrate was determined with an XFe24 Extracellular Flux Analyzer (Seahorse Bioscience), as specified by the manufacturer. Fatty acid oxidation was determined by palmitate-dependent OCR in permeabilized cells as described [42]. MEFs or fibroblasts were seeded in XFe24 cell culture microplates at the density of 7.5x10^3 cells per well. Data were normalized to the number of cells in each well counted at the end of the experiment.

2.9. Microarray analysis

RNA was extracted from liver and skeletal muscles of 6-month-old *Adck2*+/- (n=5) and WT (n=5) mice. Probe-target hybridization with GeneChip Mouse Genome Plus 2.0 (Affymetrix) was performed as we previously described [43]. Statistical analyses were performed comparing each signal of *Adck2*+/- with the corresponding signal of WT. Data have been deposited with the NCBI-GEO database at http://www.ncbi.nlm.nih.gov/geo/ with accession number GSE104996. Microarray results were validated by quantitative RT-PCR analysis of 10 significant genes (Table S7).

2.10. Untargeted metabolomics assay

Metabolomics analysis on mouse liver, skeletal muscle, and plasma extracts was performed by the UC Davis West Coast Metabolomics Center according to established procedures [43]. Twelve months-old *Adck2*+/- and WT mice were used (n=6).

2.11. Metabolic cages

Mouse metabolic rate was assessed *in vivo* by indirect calorimetry in open-circuit oxymax chambers using the Comprehensive Lab Animal Monitoring System (CLAMS; Columbus Instruments, Columbus, Ohio, US) as previously described [44].

2.12. Quantitative real-time PCR

Quantitative real-time PCR was performed to measure the expression of select target genes [45]. The primers were designed with the Beacon Designer software, and the primer pair sequences used in this study were as followed: human *ADCK2*, forward primer 5'-CAGGAAGAACACCATCAC-3' and reverse primer 5'-TGAGTCATCAGCAACTTAA-3'; mouse *Adck2*, forward primer 5'-TAAGTCAGATCACCTCAT-3' and reverse primer 5'-CAATCTTCATCAGCAGTA-3'; human *GAPDH*, forward primer 5'-TGCACACCACCAACTGCTTAGC-3' and reverse primer 5'-GGCATGGACTGTGGTCATGAG-3'; and mouse *Gapdh*, forward primer 5'-TGACGTGCCGCCTGGAGAAA-3' and reverse primer 5'-AGTGTAGCCCAAGATGCCCTTCAG-3'.

The following primer pairs were used (F, forward orientation; R, reverse orientation; sequence 5′ to 3′) to validate microarray results (Table S7): ApoA2-F (TGGTCGCACTGCTGGTAAC), ApoA2-R (TTTGCCATATTCAGTCATGCTCT), Cdx4-F (TGACATGACCTCCCCAGTTTT), Cdx4-R (GCCGGAGTCAAGAGAAACCA), Ctsh-F (ACCGTGAACGCCATAGAAAAG), Ctsh-R (TGAGCAATTCTGAGGCTCTGA), Gstp1-F (ATGCCACCATACACCATTGTC), Gstp1-R (GGGAGCTGCCCATACAGAC), Mia2-F (GTGTCTGGAGGGTACAAAGTTG), Mia2-R (TCGGGTCCTGTGTAATCTCTC), Ndufb2-F (CCCCGGTACAGGGAGTTTC), Ndufb2-R (GCCAAAATCGCCAAAGAATCCA), Phlda2-F (CTCCGACGAGATCCTTTGCG), Phla2-R (ACACGTACTTAGAGGTGTGCTC), Slc2a2-F (TCAGAAGACAAGATCACCGGA) Slc2a2-R (GCTGGTGTGACTGTAAGTGGG), Tomm7-F (ATCCGCTGGGGCTTTATTCC), Tomm7-R (CGACGGTTCAGGCATTCCA), Trf-F (GCTGTCCCTGACAAAACGGT), Trf-R (CGGAAGGACGGTCTTCATGTG).

2.13. ADCK2 silencing by siRNA

Small inhibitory RNAs (siRNA) against human *ADCK2* (Hs_ADCK2_6) were purchased from Qiagen (Hilden, Germany) and had the following sequences: sense strand 5′-GAUUGACCUGCGUUACGAA-3′, antisense strand 5′-UUCGUAACGCAGGUCAAUC-3′, and the target sequence in *ADCK2* 5′-CAGATTGACCTGTACGAA-3′. Cells were seeded in a 60-mm dish at $3.5x10^5$ cells/plate 24 h prior to transfection and were then transfected with 0.4 nmol of siRNA using oligofectamine (Invitrogen) as transfection reagent. Cells were harvested and analyzed 72 h after transfection. The knockdown of *ADCK2* was confirmed by quantitative real-time PCR

2.14. Antibodies

Primary antibodies were used against ADCK2 (custom antibody from Biomedal, 1:1000), ADCK2 (Byorbit, orb100461, 1:500), Tom20 (Santa Cruz, sc-11415, 1:10000), Opa1 (BD Biosciences, 612606, 1:1000), OAT (Acris Antibodies, AMO9362PU-S, 1:1000), Calnexin (Stressgen, ADI-SPA-860, 1:1500), Mitofusin2 (Abcam, ab50843, 1:1000) and LDH (Rockland, 100-1173, 1:2000).

2.15. Statistics

Statistical comparisons between animals of both genotypes were assessed using paired Student's *t*-test. Analyses were performed using Excel 2010 (Microsoft Corp., Redmond, WA). LogRank statistical analyses were performed using Sigmastat 3.5 (Systat Software Inc, San Jose, CA). For behavior tests, comparisons between groups were made by a Student's *t*-test, and the differences between sessions were analyzed with repeated measures ANOVA using SPSS 18 software (Madrid, Spain). Results are expressed as the mean ± SD and differences were considered significant at p values ≤ 0.05.

2.16. Study approval

We obtained blood, muscle samples, and pedigrees following informed consent from individuals of the family of the patient with severe myopathy. The Ethical Committee of the Carl Gustav Carus University, Dresden, approved human subject research. A reference pathologist evaluated muscle biopsies. The Ethical Committee for Animal Experimentation of the University Pablo de Olavide approved the mouse studies on May 27, 2014, according to the European Union Directive of 22 September 2010 (2010/63/UE) and with the Spanish Royal Decree of 1 February 2013 (53/2013). All efforts were made to minimize the number of animals used and their suffering.

3. Results

3.1. Haploinsufficiency of human ADCK2 causes defect in lipid catabolism and CoQ_{10}-deficient myopathy

The index patient, a 50-years-old male,[subject II-3 (Fig. S1A)], developed a slow, progressive proximal muscle weakness with permanent myalgia both at rest and during muscular exertion, resulting in permanent disability. Finally, the patient required a wheel chair. Muscle MRI revealed severe fatty degeneration of the shoulder girdle, deltoid, biceps, hamstring and calf muscles, whilst the triceps was well preserved (Figure S1B). The patient developed a lipid storage myopathy and liver dysfunction. Histological analysis of skeletal muscle demonstrated mitochondrial myopathy associated with lipid droplets (Fig. 1A). The patient had normal cognitive function and did not show ataxia. Analysis of a the mitochondrial genome was negative. Sequencing of a set of genes potentially involved with primary or secondary CoQ deficiency showed the heterozygous NM_052853.3:c.997C>T; p.(Arg333*) mutation in exon 2 of *ADCK2* in both the forward and reverse sequences, which was absent in 50 subjects from the same ancestry. The variant is absent among the ~13005 alleles listed on the NHLBI exome sequencing project exome variant server (http://evs.gs.washington.edu/EVS/) and is not listed on the 1000 genomes project database, and has a minor allelic frequency (MAF) of 2:251006 (http://gnomad.broadinstitute.org). Although his mother and sister harbor the same mutation, they do not currently have any neuromuscular symptoms (Fig. S1C). The mutation produced a termination codon that led to a significant decrease in ADCK2 mRNA and protein levels in dermal fibroblasts of both the patient (II-3) and his sister (II-2) (Figs. 1B-1D), which showed a significant CoQ_{10} deficiency (Fig. 1E). Both *ADCK2* mRNA levels (Fig. 1F) and CoQ_{10} content (Fig. 1G) were rescued in these cells transfected with the WT *ADCK2* allele. The activities of complexes I+III and II+III of muscle (Fig. 1H) and fibroblasts (Fig.1I) were reduced, indicative of a CoQ deficiency.

A moderate elevation in plasma levels of saturated short- and medium-chain length acyl-carnitine species was observed (Table S1, column 1), compatible with multiple acyl-CoA dehydrogenase deficiencies. Patient II-3 was treated with 75 mg CoQ_{10} per day (Fig. S1E-B) showing an improvement in the plasma lactate and myoglobin levels (Fig. S1). One month later, the patient

Peer-reviewed version available at J. Clin. Med. 2019, 8, 1374; doi:10.3390/jcm8091374

stopped taking CoQ_{10}, but after 3 weeks, his pain worsened, his muscle strength decreased, and he was unable to lift his arms, indicating that the symptoms were partially dependent on CoQ_{10}. A complete description of the pathological phenotype of the patient is presented in Supplementary information.

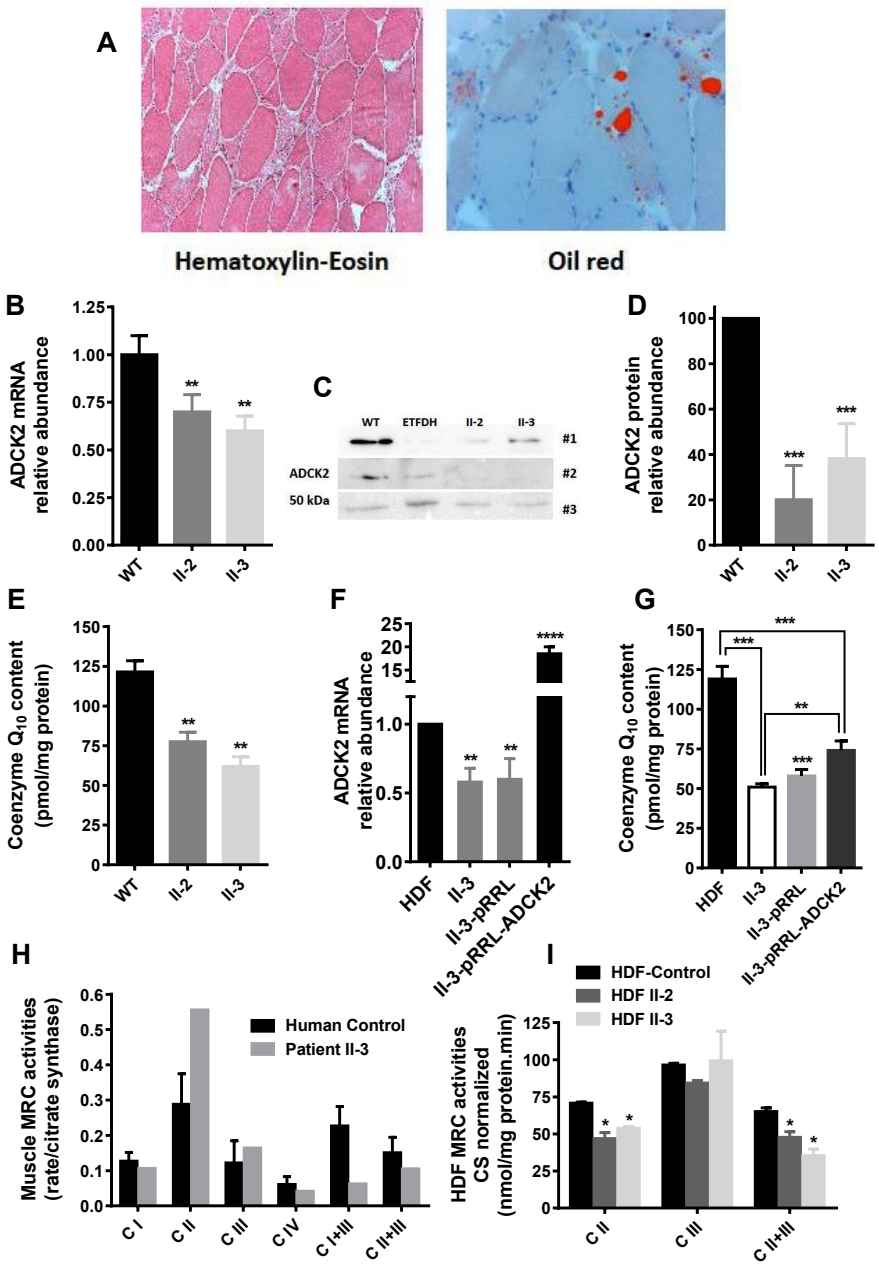

Figure 1. Laboratory findings in the index patient. A. Histological findings in muscle of patient II-3: i) some fiber atrophy and fibers containing numerous vacuoles are apparent with the haematoxylin-eosin stain (x 10); ii) Gomori trichrome stain showing lipid droplets in some muscle fibers (x 20). B. Measurement of the amount of *ADCK2* mRNA in cultured fibroblasts from II-3 and II-2 relative to controls. C. Western blotting of ADCK2 in cultured fibroblasts from II-3 and II-2. D. Quantification of the protein expression levels measured in C. E. CoQ content in dermal fibroblasts from patients II-3 and II-2 (n=5). Expression level of *ADCK2* mRNA (F) and CoQ content (G) in patient fibroblasts transformed with the *ADCK2* WT allele (n=5). H. MRC activities in patient II-3 muscle biopsy normalized to citrate synthase. The complexes III and IV values shown are $x10^{-2}$. I. MRC activities in human dermal fibroblasts from control and patients II-2 and II-3. * $p<0.05$, ** $p\leq0.01$, *** $p\leq0.005$ vs.

297 control/WT, **** $p < 0.001$ vs. non-transformed/empty vector; n=10. Data were analyzed by Student's
298 t test.

299 *3.2. A heterozygous Adck2 knockout mouse model recapitulates the phenotype observed in patient II-3.*

300 A heterozygous (*Adck2*+/-) knockout mouse model was developed based on the high homology
301 and sequence conservation of this gene across different species. The *Adck2* mRNA expression was
302 significantly lower in liver and heart, with a trend toward reduced expression in skeletal muscle but
303 without change in brain and kidney (Fig. 2A). Adck2 protein was also decreased in heart, liver and
304 skeletal muscle, but was increased in both brain and kidney as compared to wild type (WT)
305 littermates (Fig. 2B and 2C). Heterozygote pups weighted significantly less at weaning than WT
306 (*Adck2*+/-: 15.84±0.64 g (n=10), WT: 18.23±0.35 g (n=13), $p \leq 0.003$) and showed a trend toward greater
307 weight gain with age (Fig. 2D). No significant difference in body weight was noted for most of the
308 time points analyzed (Fig. S2A) despite visceral fat accumulation (Fig. S2B). Male *Adck2*+/- mice (12
309 months-old) showed significantly reduced overall endurance, characterized by shorter running
310 distance on a treadmill due to exhaustion (Fig. 2E) and poorer motor coordination as assessed by the
311 rotarod test (Fig. 2F). A decline in grip strength by both two and four limbs was also observed in the
312 mutant mice (Fig. 2G). Thus, *Adck2* deficiency causes locomotor dysfunction in mice.
313 Pathological laboratory findings in the *Adck2*+/- mice included significantly increased plasma
314 lactate (in mmol/L, 7.1±0.2 for *Adck2*+/- vs. 3.4±0.08 for WT; $p<0.05$, n=7) and accumulation of organic
315 acids in the urine (Table S2). A non-significant increase in transaminases was observed in the plasma
316 of 6-month-old mice: GPT/ALT (in mg/dL, 52.2±6.1 in WT and 56.3±5.5 in *Adck2*+/-; p=0.937, n=5) and
317 GOT/AST (in mg/dL, 464.8±120 in WT and 660.7±122 in *Adck2*+/-; p=0.426, n=5).

Peer-reviewed version available at J. Clin. Med. 2019, 8, 1374; doi:10.3390/jcm8091374

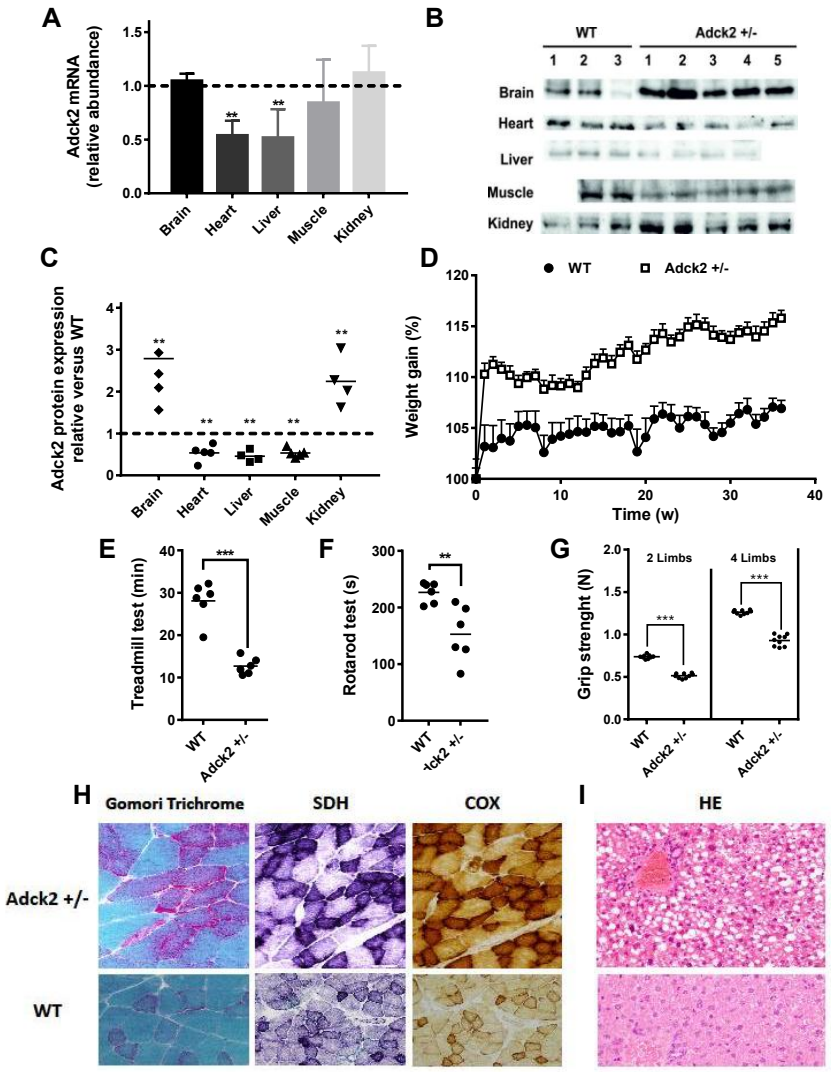

Figure 2. Characteristics of the *Adck2*+/- mouse model. A. Relative abundance of *Adck2* mRNA levels in different tissues of the *Adck2*+/- mouse after normalization to WT mice depicted as a dotted line. Bars represent mean + SD; ** p<0.01 (n=5 per group). B. Western blot of ADCK2 protein in different mouse tissues. C. Densitometry of ADCK2 protein levels from panel B (n=4-5). D. Weight gain trajectories of WT and *Adck2*+/- male mice on standard diet (n=15). E. Physical activity as determined by the running time on a treadmill until exhaustion. F. The latency period before falling off an accelerating rotarod. (G). Grip strength capacity ** p<0.01 vs. WT; *** p<0.005vs. WT; n=6. Data were analyzed by 1-way ANOVA (D) and Student's t test (panels A, B and E-G). H. Skeletal muscle of *Adck2*+/- mice stained with Gomori trichrome, succinate dehydrogenase (SDH), and cytochrome c oxidase (COX) were compared to WT; 60x magnification. I. Light microscopy of mouse *Adck2*+/- liver showing extensive steatosis compared to WT after haematoxylin and eosin (HE) staining; 40x magnification.

Gomori trichrome stain of gastrocnemius muscle from *Adck2*+/- mice showed a mild variation in fiber size, and some fibers may be classified as ragged red fibers (Fig. 2H). Both the succinate dehydrogenase (SDH) and cytochrome *c* oxidase (COX) staining were increased in *Adck2*+/- muscle fibers compared with WT (Fig. 2H), consistent with mitochondrial proliferation. Hematoxylin and eosin (H&E) analysis of liver from *Adck2*+/- mice showed an accumulation of large lipid droplets in periportal and perivenular hepatocytes compared to WT littermates (Fig. 2I).

We performed memory and neurobehavioral assessments in 12-month-old *Adck2*+/- mice. Using the hot-plate test to measure the pain response, no differences were observed in both the latency

period and the behavioral reaction to pain caused by heat (Fig. S3A), indicating unaltered nociceptive information and emotional response in the *Adck2*+/- mice. The fear-conditioning test indicated that both groups of mice entered the dark compartment with similar latencies and in the retention test WT and *Adck2*+/- mice displayed the same responses (Fig. S3A). The novel object recognition (NOR) task also evaluates short- and long-term memories. The total number of object contacts made by *Adck2*+/- mice was somewhat higher during the training session and after a latency period (Fig. S3B). Exploratory behavior of *Adck2*+/- mice in the open field apparatus also tended to be higher, but without significant difference compared to WT controls (Fig. S3B). No significant differences were observed in the Recognition Index in any session in both groups of mice (Fig. S3C). Taken together, these results demonstrate the absence of central nervous system impairment in *Adck2*+/- mice.

3.3. Adck2 deficiency causes CoQ deficiency in MEFs and skeletal muscle

Similar to the patient's fibroblasts and muscle, cultures of mouse embryonic fibroblasts (MEFs) isolated from 9 day-old *Adck2*-/- and *Adck2*+/- embryos exhibited a significant reduction in both CoQ_9 and CoQ_{10} levels (Fig. 3A) and in their biosynthetic rates as determined by the incorporation of ^{14}C-*p*hydroxybenzoate (*p*-HB) (Fig. 3B). *ADCK2* knockdown by siRNA interference induced a significant decrease in CoQ biosynthesis rate in human MRC5 cells, confirming the role of *ADCK2* in CoQ biosynthesis (Fig. 3C). The rate of incorporation of the isoprenoid moiety in CoQ was measured by incubating MEFs with ^{3}H-mevalonate in the presence of an excess of non-labeled *p*-HB. Regardless of the genotype, the levels of radiolabeled CoQ and cholesterol were unchanged in total MEF homogenates, whereas the mitochondrial fraction of *Adck2*-deficient MEFs had significantly lower levels of both molecules, indicating a defect in intracellular trafficking into mitochondria of isoprenoid and cholesterol from cytoplasm, where they are synthesized *de novo* (Fig. 3D).

Complementation assays in *Saccharomyces cerevisiae* null strains have been employed to validate *ADCK2* in CoQ biosynthesis. The deletion of *YPL109c*, the *S. cerevisiae* homolog of human *ADCK2*, caused a 40% decrease in the production of CoQ_6, the specific isoform in yeast (Fig. 3E). Transformation of the *ΔYPL109c* yeast strain with wild type *YPL109c* or human *ADCK2* construct rescued CoQ_6 biosynthesis, whereas a mutant allele with a stop codon or the yeast gene with an equivalent stop codon failed to complement the mutant strain (Fig. 3E).

CoQ_9 and CoQ_{10} concentrations were also significantly lower in skeletal muscle of *Adck2*+/- mice compared to WT, with a downward trend in the heart and liver but not in the brain or kidney of *Adck2*+/- animals (Figs. 3F, 3G). Collectively, these results support the role of *ADCK2*-encoded protein in the biosynthesis of mitochondrial CoQ in both mammal and yeast cells, mainly affecting skeletal muscle of *Adck2*+/- mice.

Peer-reviewed version available at J. Clin. Med. 2019, 8, 1374; doi:10.3390/jcm8091374

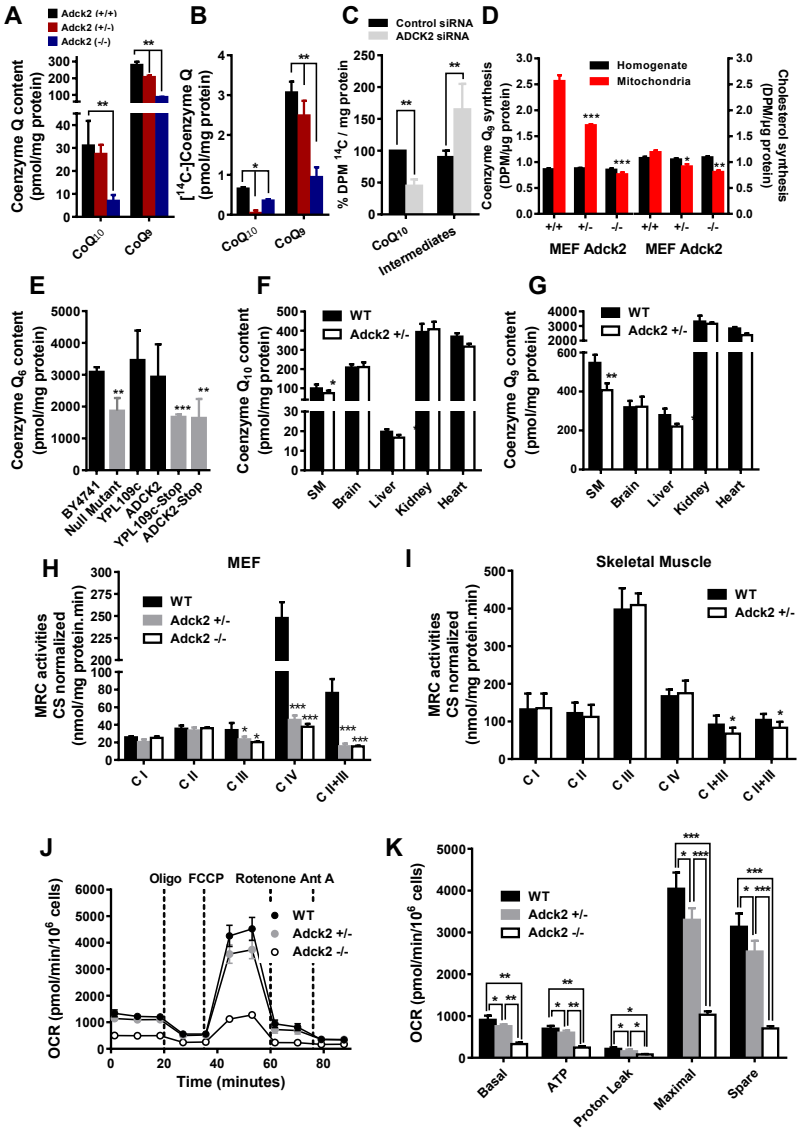

Figure 3. Coenzyme Q content and MRC activities in cells and tissues. CoQ_9 and CoQ_{10} content (A) and biosynthesis (B) in MEFs isolated from Adck2-/-, *Adck2*+/- and WT mice (n=5). C. Effect of siRNA silencing of *ADCK2* in MRC5 human fibroblasts on the rate of CoQ_{10} biosynthesis measured by the incorporation of ^{14}C-*p*-HB intermediate (n=4). D. Levels of CoQ and cholesterol produced in the presence of ^{3}H-mevalonate in total homogenate and mitochondria fractions from MEFs. E. CoQ_6 content in BY4741 WT and *ΔYPL109c* (null mutant) yeast strains after transformation of ΔYPL109c with *YPL109c* WT or human *ADCK2*. Also, *ΔYPL109c* was transformed with mutant alleles of either *YPL109c* (*YPL109c*-stop) or *ADCK2* (ADCK2-stop) (n=7). The content in CoQ_{10} (F) and CoQ_9 (G) was determined in various tissues and organs of *Adck2*+/- and WT mice (n=5). MRC activities normalized to citrate synthase in MEFs (H) and skeletal muscle (I) of both WT and *Adck2*+/- mice. J and K. OCR in WT, Adck2+/- and *Adck2*-/- MEFs. Bars are mean + SD. Data was analyzed by Student's t test. (n=5); * p< 0.05, **p< 0.01, and ***p< 0.005 vs. WT.

3.4. Adck2 haploinsufficiency causes mitochondrial dysfunction

Immunoblot analysis of ADCK2 in various subcellular fractions obtained from HEK293 cells showed a distribution similar to the mitochondrial TOM20 and Mfn2 (Figs. S4A and S4B). The presence of ADCK2 was not detected in the endoplasmic reticulum and cytosolic fractions. A proteinase K protection assay in mitochondrial-enriched fractions (MAM) of HEK293 cells revealed that the outer mitochondrial protein TOM20, and the MAM/endoplasmic reticulum protein calnexin were susceptible to proteinase K treatment, whilst the inner mitochondrial membrane protein OPA1,

the matrix protein ornithine aminotransferase, and ADCK2 were resistant to this treatment. The susceptibility of the ADCK2 protein to proteinase K treatment following disruption of the mitochondria by treatment with the detergent Triton X-100 indicates its presence in the mitochondrial matrix or bound to the inner mitochondrial membrane (Fig. S4C).

The urinary excretion of organic acids, such as lactate, was significantly increased in *Adck2*+/- mice (Table S2), as was the blood lactate level (in mmol/L, 7.1±0.2 for *Adck2*+/- versus 3.4±0.08 for WT; $p<0.05$, $n=7$), indicating mitochondrial dysfunction. MEFs isolated from mutant mice embryos showed a significant decrease in mitochondrial complexes III, II+III, and IV activities (Fig. 3H). Mitochondrial complex I+III and II+III activities were significantly decreased in *Adck2*+/- skeletal muscle, but the activities of the individual complexes were normal (Fig. 3I). In contrast, complex I, II, and I+III activities were significantly higher in kidney mitochondria of *Adck2*+/- mice, whilst those of complex III, IV, and II+III were not affected (Fig. S5A). The mitochondrial respiratory complexes were unaffected in the brain and liver of *Adck2*+/- mice (Figs. S5B and S5C). The analysis of oxygen consumption rate (OCR) using the Seahorse XF Extracellular Flux Analyzer showed a significant difference in basal and maximum respiration in WT compared to *Adck2*+/- and *Adck2*-/- MEFs when glucose was used as substrate (Figs. 3J and 3K). Taken together, these data suggest that ADCK2 deficiency impairs the normal MRC function in MEFs and skeletal muscle mitochondria ultimately leading to mitochondrial dysfunction.

3.5. Adck2 haploinsufficiency decreases mitochondrial fatty acid β-oxidation

To compare with the patient's phenotype, fatty acid oxidation was analyzed in *Adck2*+/- mice. As anticipated, the growth of WT and *Adck2*+/- MEFs was reduced when incubated in a medium with low glucose (e.g. 1 g/L glucose) (Fig. 4A). The addition of fatty acids to a glucose-containing growth medium increased the proliferation of WT, but not mutant MEFs, whereas fatty acid supplementation in glucose-free medium caused more than 50% growth arrest of mutant MEFs compared to WT cells (Fig. 4A). Supplementation with 30μM CoQ significantly increased coupled OCR in mutant MEFs (Fig. 4B), indicating the requirement of CoQ for fatty acid-dependent respiration in MEFs. These results indicate that ADCK2 is required to meet the energy demands by fatty acid β-oxidation of these cells. Accordingly, palmitate-dependent OCR in permeabilized MEFs decreased in *Adck2* mutant MEFs compared to WT (Figs. 4B).

β-Hydroxybutyrate was decreased in plasma of *Adck2*+/- mice compared to WT (Fig. 4C) that correlates with defective mitochondrial fatty acid oxidation [46]. Here, circulating fatty acids of male *Adck2*+/- mice showed a significant decrease of free carnitine while short- and long-chain fatty acid levels were present at higher concentrations compared to WT (Fig. 4D), confirmed by the significantly higher urinary excretion of adipic and ethylmalonic acids in *Adck2*+/- mice (Table S2). These results resemble the impaired fatty acid phenotype of the participant patient.

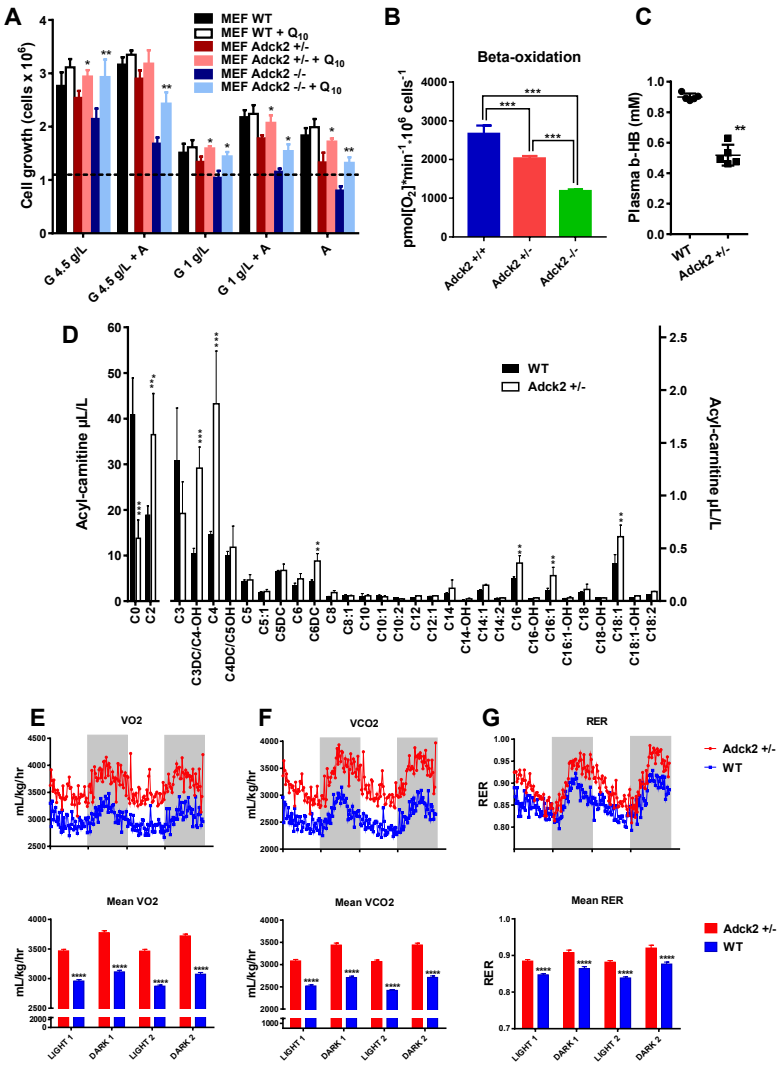

Figure 4. Metabolic changes associated with *Adck2* insufficiency. A. Effect of glucose compared to fatty acids as carbon source on MEFs proliferation. MEFs were grown in high glucose (4.5g/L), low glucose (1g/L) or 1 mg/ml fatty acids (AlbuMax©) media for 72 h supplemented or not with 30nM CoQ_{10}. * p=0.05, ** p≤0.01vs. non-supplemented; (n=5). C. Content of β-hydroxybutyrate in the plasma of *Adck2*+/- and WT mice. **p≤0.01 vs. WT. D. Acyl-carnitine profile measured in plasma of WT and *Adck2*+/- mice. ** p≤0.01, *** p≤0.005 vs. WT. E. Metabolic cages analysis of O_2 consumption, CO_2 production, and respiratory exchange ratio (RER) during two fed-fasted periods comparing *Adck2*+/- and WT mice (n=6). **** p < 0.001 vs. WT. Data were analyzed by Student's t test.

To further characterize the energy expenditure by both phenotypes we used the indirect respiration calorimetry system (CLAMS metabolic chamber) to determine the preferential use of fat or carbohydrates for their energy needs [44]. *Adck2*+/- mice showed significantly higher oxygen consumption (Fig. 4E), CO_2 production (Fig. 4F), and RER (~0.9) (Fig. 4G) as compared to WT that had a RER of ~0.85. These data are consistent with greater use of carbohydrates by the mutant mice and consumption of a mix of fat and carbohydrates by the WT (Fig. 4G).

3.6.Adck2haploinsufficiency affects gene expression profile in muscle and liver

To further characterize the effect of *Adck2* haploinsufficiency, we performed microarray assays of RNA isolated from skeletal muscle and liver of WT and *Adck2*+/- mice. Heat map analysis showed extensive changes in the global transcript expression levels between WT and *Adck2*+/- in these tissues (Figs. S6A and S6B). Principal component analysis based on significant Z-scores demonstrated a clear effect of *Adck2* haploinsufficiency in muscle (Fig. 5A) and liver (Fig. 5C). Ingenuity pathway analysis

indicated a robust induction in the expression of genes related to muscle development and different myopathic conditions upon *Adck2* depletion (Fig. 5B, Table S3). Major regulated genes included several biomarkers of muscle diseases, such as *Car3*, *Fbxo32*, and *Ttid*, which are overexpressed in Duchene muscle dystrophy and muscle atrophy. Additionally, *Gde1*, which is involved in skeletal muscle development, *Pdlim5*, a promoter of cardiac hypertrophy, and *Ppp1cb*, a regulator of cell division, glycogen metabolism, and muscle contractility were overexpressed. Among the repressed genes included those implicated in muscle contractility such as *Phpt1* and *Fxyd1*. Several subunits of both cytosolic and mitochondria ribosomes (*Rps26*, *Mrpl52* and *Rpl28*) and genes related to the control of cell proliferation, apoptosis, and mitochondrial morphology (*Romo1* and *Lgals1*) were also repressed in *Adck2*+/- muscle. Gene Ontology enrichment analysis demonstrated that mitochondrial metabolism was affected and diverse ion transport pathways with concomitant repression in the activities of mitochondrial respiratory complexes, ribosomes, and protein synthesis (Table S4). Figure S6C summarizes the metabolic pathways affected by *Adck2* insufficiency in mouse skeletal muscle based on the information obtained from microarrays (Table S4).

Among the most significantly activated genes in the liver of *Adck2*+/- mice (Table S5) were four cytochrome P450s, two genes related with lipoproteins (*Vldlr*, *Srebp2*), a number of genes involved in the metabolism of cholesterol (*Mvd*), fatty acids (*Aacs*, *Acot1*, *Acot2*, *Acot4*, *Crat*, *Elovl1*, *Fasn*) and other organic acids (*Pgpep1*, *Pdk4*). Gene ontology analysis showed a general activation of fatty acid metabolism (Fig. 5D, Table S6), which could explain the liver steatosis in *Adck2*+/- mice. There was also an enrichment of genes associated with the metabolism of organic acid, purine and cholesterol. Top down-regulated genes featured those implicated both in the repression of interleukin production and inactivation of the JNK pathway, consistent with activation of the hepatic inflammatory response (Fig. 5D. Table S6). Expression of the DNA methyltransferase *Dnmt3b* was significantly higher and that of *Gstp1* was significantly lower in the *Adck2*+/- liver, supporting the idea of an uptick in hepatic inflammation [47]. Microarray gene expression profiles in muscle and liver were validated by quantitative real-time PCR (Table S7).

3.7. Adck2 haploinsufficiency affects metabolomics profile

To better understand the metabolic adaptation of mice to *Adck2* insufficiency, we performed untargeted metabolomics in the liver, plasma and skeletal muscle of 12-month-old mice of both genotypes. Metabolite profile was compatible with mitochondrial dysfunction in skeletal muscle and defective mitochondrial fatty acid oxidation in the liver and muscle of *Adck2*+/- mice (Fig. 5E).

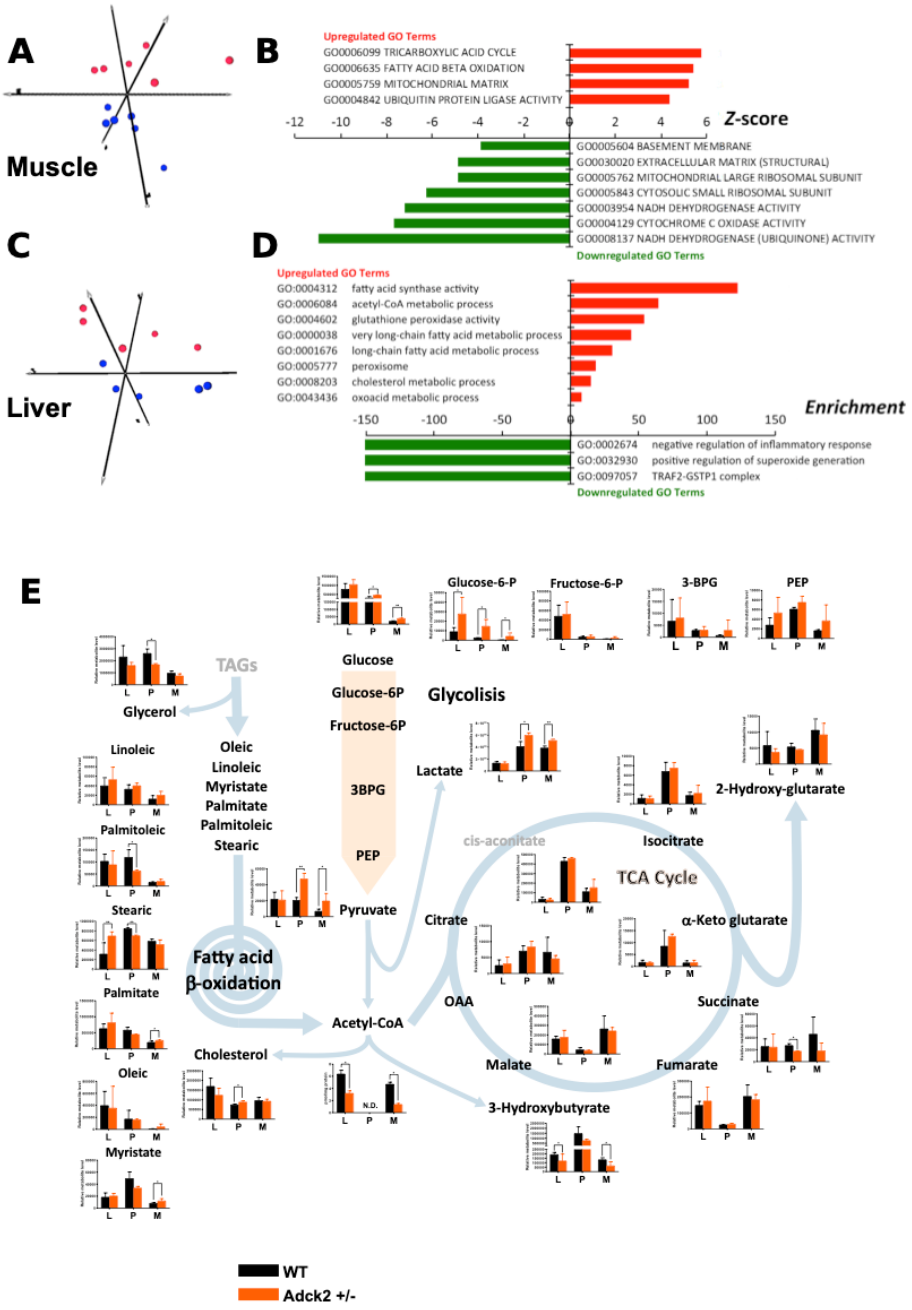

Figure 5. Transcriptome and metabolomics analyses in *Adck2*+/- mice. A. Principal component analysis from microarray results in skeletal muscle of *Adck2*+/- (red symbols) and WT (blue symbols) mice (n=6 per group). B. Bars depict GO pathways significantly regulated in skeletal muscle of *Adck2*+/- vs. WT animals. C. Principal component analysis from microarray results in liver of *Adck2*+/- (red) and WT (blue) mice (n=6 per group). D. Bars depict GO pathways significantly regulated in liver of *Adck2*+/- vs. WT animals. E. Metabolite profiles in skeletal muscle (M), liver (L), and plasma (P) of *Adck2*+/- and WT mice at 12 months of age are depicted. Results indicate major affected components of the glycolysis and fatty acid oxidation pathways, as well as the Krebs cycle (n=6 per group). Acetyl-CoA was determined independently by HPLC in liver and skeletal muscle. N.D. Non determined. All data are n=5-6 biological replicates per experimental group. *p<0.05, **p<0.01 vs. WT. Data were analyzed by Student's t test.

Accumulation of pyruvate and lactate in plasma and skeletal muscle of the mutant mice was consistent with mitochondrial dysfunction, which decreased acetyl-CoA availability for the Krebs cycle in muscle and liver (Fig. 5E). Moreover, increase in glycolysis was evident by the significant

Peer-reviewed version available at J. Clin. Med. 2019, 8, 1374; doi:10.3390/jcm8091374

accumulation of glucose and glucose-6-phosphate, along with a positive trend toward other glycolytic intermediates. The decrease in the Krebs cycle intermediate succinate, a mitochondrial complex II substrate and novel regulator of metabolic signaling [48], is worth of mention.

The defect in mitochondrial fatty acid β-oxidation in *Adck2*+/- mice (Fig. 4) was consistent with the significant decrease of β-hydroxybutyrate and glycerol, and a trend of cholesterol increase in plasma of *Adck2*+/- mice supported a lipid metabolism disorder. This was further evidenced by the accumulation of free fatty acids such as linoleic, myristic and palmitic in tissues [notably stearic acid in the liver] and their decrease in plasma. Such bioenergetics defects in *Adck2*+/- mice may explain the *in vivo* metabolic cage data (Fig. 4G).

3.8. CoQ supplementation partially rescues the Adck2+/- phenotype

The effect of CoQ_{10} supplementation in *Adck2*+/- mice was carried out to determine whether CoQ deficiency *per se* contributed to the overall phenotypic changes. Daily treatment of male *Adck2*+/- mice with 15 mg/kg CoQ_{10} for three months induced a significant decrease in plasma lactate levels (Fig. 6A), significantly improved the treadmill endurance exercise time (Fig. 6B), and also significantly increased grip strength (Fig. 6C). These effects were confirmed by the significant incorporation of CoQ_{10} in *Adck2*+/- skeletal muscle, but not in WT skeletal muscle (Fig. 6D).

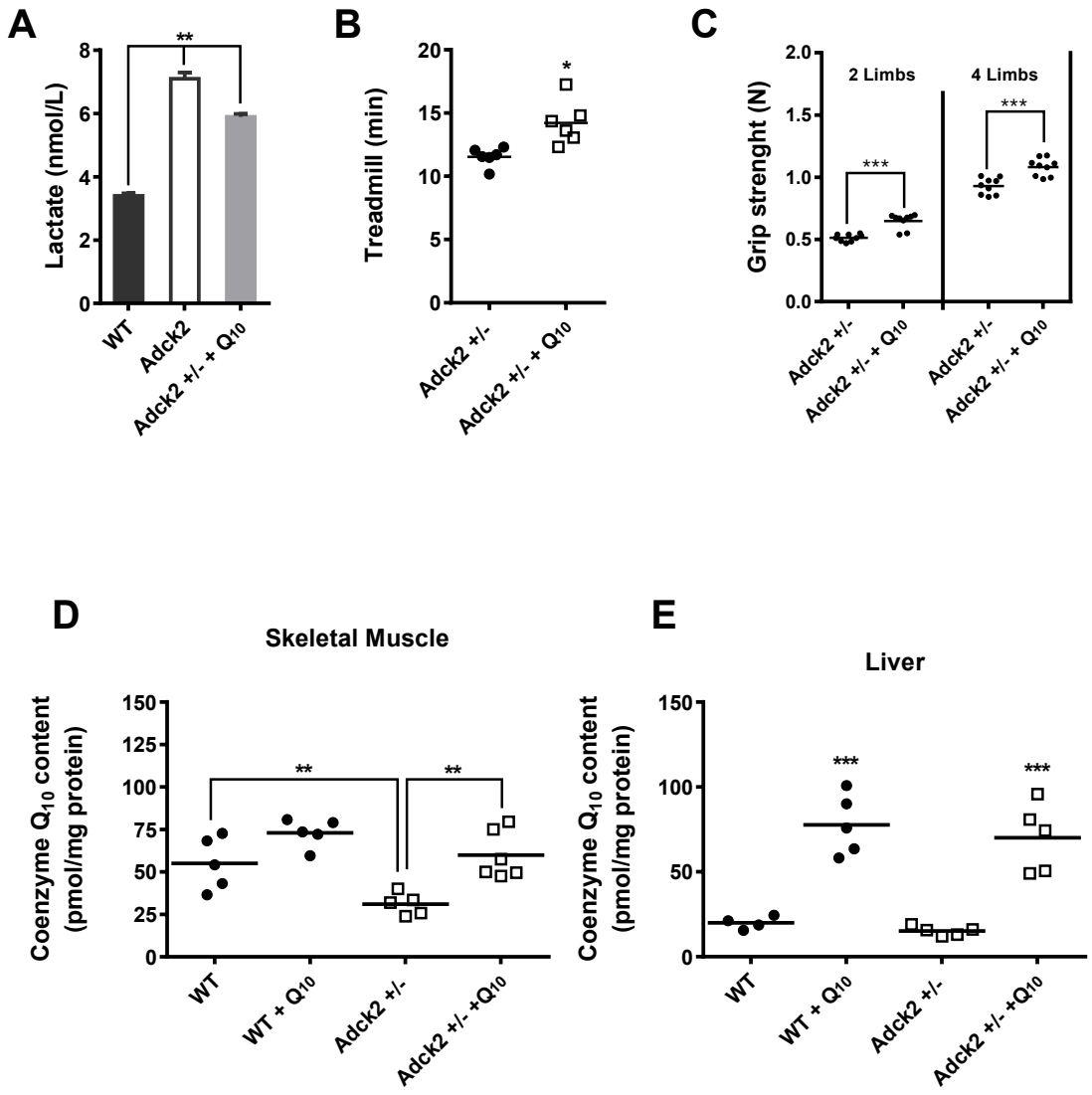

Figure 6. Supplementation with CoQ_{10} partially rescues the *Adck2*+/- phenotype. A. Six-month-old *Adck2*+/- mice were treated or not with 15 mg/kg of CoQ daily for 3 months followed by the

determination of plasma lactate. B. Running capacity on treadmill. C. Grip strength (n=6). CoQ_{10} content in skeletal muscle (D) and liver (E) of both WT and *Adck2*+/- mice in the absence and presence of CoQ supplementation (n=7). * p≤0.05, ** p≤0.01, *** p≤0.005 vs. non-treated animals. Data were analyzed by Student's t test.

Supplementation also induced an increase of CoQ_{10} in liver of both *Adck2*+/- and WT mice (Fig. 6E). CoQ supplementation caused a ~11% reduction in liver transaminases in *Adck2*+/- mice, although it did not reach statistical significance: GPT/ALT (in mg/dL, 50.5±4.7 in CoQ-treated vs. 56.3±5.5 in non-treated; p=0.851, n=7) and GOT/AST (in mg/dL, 578±120 in CoQ-treated vs. 660.7±122 in non-treated; p=0.236, n=7). These results demonstrate a partial role of CoQ deficiency in the pathogenesis of the *Adck2*+/- mouse myopathy and liver dysfunction.

4. Discussion

In the work herein, we have demonstrated the role of *ADCK2* gene in the biosynthesis of CoQ and the impact that a heterozygous nonsense mutation in *ADCK2* has on mitochondrial function in skeletal muscle of a patient and in a mouse model and on the rate of FA oxidation. A nonsense mutation in one *ADCK2* allele leads to the development of severe mitochondrial myopathy in a human patient that appears responsive to CoQ supplementation.

The sister of this patient also harbors the *ADCK2* mutation but she does not complain of neuromuscular symptoms at this time. Nevertheless, she diplays CoQ deficiency in cultured fibroblasts. Adult onset autosomal dominant diseases often display incomplete penetrance and variable expressivity. This is consistent with the detection of the same *ADCK2* mutation in two apparently healthy controls in the gnomAD database. Several factors may act as phenotype modifiers in dominant disorders. In case of facioscapulohumeral dystrophy, estrogens appear to have a protective role [49], but many other genetic and environmental factors may influence the phenotype.

There are at least two reports of patients with isolated myopathy associated with muscle CoQ deficiency and abnormal acyl-carnitine profile in the absence of brain involvement [50,51], both were isolated cases as our patient, and a definite genetic diagnosis was never achieved.

All participating proteins in the CoQ biosynthesis pathway are nuclear-encoded and are differentially expressed in various tissues and organs, and CoQ content in liver and muscle can fluctuate in response to nutritional or other stressful conditions [52,53]. *ADCK2* is demonstrated here to participate in this pathway and its deficiency in mice worsens physical performance, consistent with muscle dysfunction without behavioral abnormalities [35], resembling the phenotype of the patient. CoQ deficiency is produced as a secondary consequence of defects in components of either oxidative phosphorylation or other mitochondrial pathways [14,54]. There is evidence for tissue-specific expression and function of various members of the *ADCK* family. Mutations in *COQ8A* and *COQ8B* (previously known as *ADCK3* and *ADCK4)* have been shown to induce a decrease of CoQ in the cerebellum and kidney causing cerebellar ataxia and nephrotic syndrome, respectively [13,18,27]. Interestingly, Mfn2 has been demonstrated to contribute to the maintenance of the mitochondrial CoQ pool [11] and regulation of phospholipid transport into mitochondria through mitochondrial-associated membranes [55], in which both Mfn2 and ADCK2 colocalize (Fig. S4). Furthermore, yeast strains lacking components of the endoplasmic reticulum-mitochondria encounter structure (ERMES) showed destabilization of the CoQ_6 biosynthesis complex (synthome), leading to impaired synthesis and depletion of mitochondrial CoQ_6 pool [56]. We have also shown that MEFs depend on Adck2 for the mitochondrial availability of mevalonate-derived isoprenoid side chain of CoQ and cholesterol, which would indicate its role in lipid transport into mitochondria.

Impairment in lipid metabolism associated with defects in both hepatic and skeletal muscle functions were observed in the patient and in *Adck2* +/- mice. Defects in mitochondrial FA oxidation impair physical performance, causing exercise intolerance and reduced strength [57,58]. The mechanism by which *ADCK2* haploinsufficiency alters fatty acid catabolism implicates the accumulation of long- and short-chain fatty acids with lower free carnitine levels as noted in the plasma of the study participant and *Adck2*+/- mice. Substantial alterations in the urinary excretion of

metabolites linked to the Krebs cycle and fatty acid β-oxidation were found in mutant mice along with significant reduction in circulating β-hydroxybutyrate, which is derived from β–oxidation. Muscle-specific deletion of acyl-CoA synthetase isoform-1 (*Acsl1*$^{M-/}$) or carnitine palmitoyltransferase-1 (*Cpt1b*$^{M-/-}$) in mice reduces physical activity combined with higher circulating non-esterified fatty acids and mitochondrial dysfunction [59,60]. *Cpt1b*$^{M-/-}$ mice also show a metabolic adaptation and remodeling of glucose metabolism at a much lower extent than when amino acids are used as fuel [59,61]. Similarly, *Acsl1*$^{M-/-}$ mice are severely hypoglycemic and have poor physical endurance combined with an increase in protein catabolism [60,62]. We have also shown that Adck2 deficiency causes defects in pathways of glucose metabolism in the liver and muscle and in MEFs, as evidenced by plasma lactate accumulation, decreased in respiration , , and metabolomics data. The notion that Adck2 participates in skeletal muscle energy homeostasis is supported by the comparative transcriptome and metabolome analysis of muscle in WT and *Adck2*+/- mice together with measurement of mitochondrial activities in muscle fibers.

Moreover, liver microarray analysis and metabolomics profile enabled the identification of genes and metabolites impacted by *Adck2* insufficiency, ultimately leading to mitochondrial dysfunction. These genes were associated with fatty acid metabolism and Krebs cycle enzymes, similar to mice fed a high-fat diet [63], detoxification pathways, mainly implicating P450 genes, and the activation of inflammatory response via interleukin production and JNK pathway activation [64].

Defects in β-oxidation and CoQ biosynthesis in response to *ADCK2* depletion indicate the importance of this gene in pathways involved in mitochondrial fatty acid oxidation and in skeletal muscle metabolic regulation. The fact that CoQ supplementation partially improved plasma lactate and physical performance in human and *Adck2*+/- mice indicates that deficiency in CoQ is an important factor contributing to the phenotype reported in this study.

In conclusion, *ADCK2* haploinsufficiency causes an adult onset myopathy with CoQ deficiency, and an overall defect in mitochondrial lipid metabolism, with incomplete penetrance. The heterozygous inactivation of *Adck2* in mouse model recapitulates the human disease.ADCK2 is proposed to participate in the control of mitochondrial fatty acid oxidation and CoQ biosynthesis in skeletal muscle. We speculate that ADCK2 participates in these two pathways affecting the transport of lipids into mitochondria as isoprenoids side chain for CoQ structure and fatty acids for its degradation. From a clinical point of view, isolated myopathies and myopathies with lipid accumulation should be tested for this *ADCK2* gene defect because they are likely to be responsive to CoQ supplementation.

Supplementary Materials: The following are available online, Figure S1: Laboratory findings in the index patient, Figure S2: Adck2+/- mouse phenotype, Figure S3: *Behavioral properties of Adck2+/- mice,* Figure S4: DCK2 *protein is located inside mitochondria,* Figure S5: *Mitochondria properties of mouse tissues*, , Figure S6: Microarray analysis in mouse skeletal muscle and liver, Table S1: Acyl-carnitine analysis in plasma from the index patient II-3, Table S2: Metabolites (mmol/mol creatinine) in urine of Adck2+/- and WT mice. (Reference internal standard ion: undecanodioic, 345), Table S3: Regulated genes in Adck2+/- mouse skeletal muscle, Table S4: Gene Ontologies affected by Adck2 haploinsufficiency in mouse muscle, Table S5: Regulated genes in Adck2+/- mouse liver, **Table S6:** Gene Ontologies affected by *Adck2* haploinsufficiency in mouse liver, **Table S7:** Validation of gene expression analysis by quantitative real-time PCR.

Author Contributions: LV-F, CS-O, IN-E, IG, MVC, AS-C, ES, PG, ABC-R, JCR-A, ZH performed various biochemical analyses in cells and tissues. Mitochondrial localization experiments were carried out by LS. Metabolite and lipid analyses in mice were done by AR and RA. ZH performed DNA and RNA sequencing of the patient and family members. JS was responsible for the clinical investigations and SJ organized and participated in the molecular and biochemical studies in the patient and his family. CJ performed histological analysis in mice. IN-E executed physical fitness testing in mice while the behavior tests were performed by SJP-S and ED-d-T. GB-C and CM developed CoQ supplementation experiments and tissue incorporation of CoQ. JDH-C and GL-L performed hepatic studies. DMF-A, ADF and RdC carried out microarray analysis and interpretation of data. MB, SJ and PN wrote and edited the manuscript. PN coordinated the work and designed the mouse model.

Funding: This research was supported by grants from the Spanish Ministry of Health, Instituto de Salud Carlos III (ISCIII), PI17/01286 and Andalussian Government Excellence grant P12-CTS-943 to P. Navas, FIS PI17/00190

to R. Artuch, by grants from IRP Città della Speranza and Telethon Italy (GGP13222 and GGP14187c) to L. Salviati, and the Intramural Research Program of NIA/NIH (M.A. Aon, M. Bernier and R. de Cabo). L. Vázquez-Fonseca doctoral thesis was directed by C. Santos-Ocaña. I. Navas-Enamorado and A. di Francesco were postdoctoral fellows at NIA/NIH.

Acknowledgments: The authors thank the patient and his family for their participation. We would also like to thank GeriMed for their kind gift of ubiquinol to the patient.

Conflicts of Interest: The authors declare no competing financial interest.

References

1. Smith, R.L.; Soeters, M.R.; Wust, R.C.I.; Houtkooper, R.H. Metabolic Flexibility as an Adaptation to Energy Resources and Requirements in Health and Disease. *Endocr Rev* **2018**, *39*, 489-517, doi:10.1210/er.2017-00211.
2. Mitchell, S.J.; Bernier, M.; Mattison, J.A.; Aon, M.A.; Kaiser, T.A.; Anson, R.M.; Ikeno, Y.; Anderson, R.M.; Ingram, D.K.; de Cabo, R. Daily Fasting Improves Health and Survival in Male Mice Independent of Diet Composition and Calories. *Cell Metab* **2019**, *29*, 221-228 e223, doi:10.1016/j.cmet.2018.08.011.
3. Alcazar-Fabra, M.; Navas, P.; Brea-Calvo, G. Coenzyme Q biosynthesis and its role in the respiratory chain structure. *Biochim Biophys Acta* **2016**, *1857*, 1073-1078, doi:10.1016/j.bbabio.2016.03.010.
4. Kuzmiak-Glancy, S.; Willis, W.T. Skeletal muscle fuel selection occurs at the mitochondrial level. *J Exp Biol* **2014**, *217*, 1993-2003, doi:10.1242/jeb.098863.
5. Lapuente-Brun, E.; Moreno-Loshuertos, R.; Acin-Perez, R.; Latorre-Pellicer, A.; Colas, C.; Balsa, E.; Perales-Clemente, E.; Quiros, P.M.; Calvo, E.; Rodriguez-Hernandez, M.A., et al. Supercomplex assembly determines electron flux in the mitochondrial electron transport chain. *Science* **2013**, *340*, 1567-1570, doi:10.1126/science.1230381.
6. Grunert, S.C. Clinical and genetical heterogeneity of late-onset multiple acyl-coenzyme A dehydrogenase deficiency. *Orphanet journal of rare diseases* **2014**, *9*, 117, doi:10.1186/s13023-014-0117-5.
7. Chokchaiwong, S.; Kuo, Y.T.; Hsu, S.P.; Hsu, Y.C.; Lin, S.H.; Zhong, W.B.; Lin, Y.F.; Kao, S.H. ETF-QO Mutants Uncoupled Fatty Acid beta-Oxidation and Mitochondrial Bioenergetics Leading to Lipid Pathology. *Cells* **2019**, *8*, doi:10.3390/cells8020106.
8. Gempel, K.; Topaloglu, H.; Talim, B.; Schneiderat, P.; Schoser, B.G.; Hans, V.H.; Palmafy, B.; Kale, G.; Tokatli, A.; Quinzii, C., et al. The myopathic form of coenzyme Q10 deficiency is caused by mutations in the electron-transferring-flavoprotein dehydrogenase (ETFDH) gene. *Brain* **2007**, *130*, 2037-2044, doi:10.1093/brain/awm054.
9. Liang, W.C.; Ohkuma, A.; Hayashi, Y.K.; Lopez, L.C.; Hirano, M.; Nonaka, I.; Noguchi, S.; Chen, L.H.; Jong, Y.J.; Nishino, I. ETFDH mutations, CoQ10 levels, and respiratory chain activities in patients with riboflavin-responsive multiple acyl-CoA dehydrogenase deficiency. *Neuromuscul Disord* **2009**, *19*, 212-216, doi:10.1016/j.nmd.2009.01.008.
10. Wen, B.; Li, D.; Shan, J.; Liu, S.; Li, W.; Zhao, Y.; Lin, P.; Zheng, J.; Li, D.; Gong, Y., et al. Increased muscle coenzyme Q10 in riboflavin responsive MADD with ETFDH gene mutations due to secondary mitochondrial proliferation. *Mol Genet Metab* **2013**, *109*, 154-160, doi:10.1016/j.ymgme.2013.04.007.
11. Mourier, A.; Motori, E.; Brandt, T.; Lagouge, M.; Atanassov, I.; Galinier, A.; Rappl, G.; Brodesser, S.; Hultenby, K.; Dieterich, C., et al. Mitofusin 2 is required to maintain mitochondrial coenzyme Q levels. *The Journal of cell biology* **2015**, *208*, 429-442, doi:10.1083/jcb.201411100.
12. Gorman, G.S.; Chinnery, P.F.; DiMauro, S.; Hirano, M.; Koga, Y.; McFarland, R.; Suomalainen, A.; Thorburn, D.R.; Zeviani, M.; Turnbull, D.M. Mitochondrial diseases. *Nature reviews. Disease primers* **2016**, *2*, 16080, doi:10.1038/nrdp.2016.80.
13. Salviati, L.; Trevisson, E.; Doimo, M.; Navas, P. Primary Coenzyme Q10 Deficiency. In *GeneReviews(R)*, Pagon, R.A., Adam, M.P., Ardinger, H.H., Wallace, S.E., Amemiya, A., Bean, L.J.H., Bird, T.D., Ledbetter, N., Mefford, H.C., Smith, R.J.H., et al., Eds. Seattle (WA), 2017.
14. Kuhl, I.; Miranda, M.; Atanassov, I.; Kuznetsova, I.; Hinze, Y.; Mourier, A.; Filipovska, A.; Larsson, N.G. Transcriptomic and proteomic landscape of mitochondrial dysfunction reveals secondary coenzyme Q deficiency in mammals. *Elife* **2017**, *6*, doi:10.7554/eLife.30952.
15. Yubero, D.; Montero, R.; Martin, M.A.; Montoya, J.; Ribes, A.; Grazina, M.; Trevisson, E.; Rodriguez-Aguilera, J.C.; Hargreaves, I.P.; Salviati, L., et al. Secondary coenzyme Q10 deficiencies in oxidative phosphorylation (OXPHOS) and non-OXPHOS disorders. *Mitochondrion* **2016**, *30*, 51-58, doi:10.1016/j.mito.2016.06.007.

16. Vazquez Fonseca, L.; Doimo, M.; Calderan, C.; Desbats, M.A.; Acosta, M.J.; Cerqua, C.; Cassina, M.; Ashraf, S.; Hildebrandt, F.; Sartori, G., et al. Mutations in COQ8B (ADCK4) found in patients with steroid-resistant nephrotic syndrome alter COQ8B function. *Hum Mutat* **2018**, *39*, 406-414, doi:10.1002/humu.23376.
17. Xie, L.X.; Hsieh, E.J.; Watanabe, S.; Allan, C.M.; Chen, J.Y.; Tran, U.C.; Clarke, C.F. Expression of the human atypical kinase ADCK3 rescues coenzyme Q biosynthesis and phosphorylation of Coq polypeptides in yeast coq8 mutants. *Biochim Biophys Acta* **2011**, *1811*, 348-360, doi:10.1016/j.bbalip.2011.01.009.
18. Stefely, J.A.; Licitra, F.; Laredj, L.; Reidenbach, A.G.; Kemmerer, Z.A.; Grangeray, A.; Jaeg-Ehret, T.; Minogue, C.E.; Ulbrich, A.; Hutchins, P.D., et al. Cerebellar Ataxia and Coenzyme Q Deficiency through Loss of Unorthodox Kinase Activity. *Mol Cell* **2016**, *63*, 608-620, doi:10.1016/j.molcel.2016.06.030.
19. Stefely, J.A.; Reidenbach, A.G.; Ulbrich, A.; Oruganty, K.; Floyd, B.J.; Jochem, A.; Saunders, J.M.; Johnson, I.E.; Minogue, C.E.; Wrobel, R.L., et al. Mitochondrial ADCK3 Employs an Atypical Protein Kinase-like Fold to Enable Coenzyme Q Biosynthesis. *Mol Cell* **2015**, *57*, 83-94, doi:10.1016/j.molcel.2014.11.002.
20. Blumkin, L.; Leshinsky-Silver, E.; Zerem, A.; Yosovich, K.; Lerman-Sagie, T.; Lev, D. Heterozygous Mutations in the ADCK3 Gene in Siblings with Cerebellar Atrophy and Extreme Phenotypic Variability. *JIMD reports* **2014**, *12*, 103-107, doi:10.1007/8904_2013_251.
21. Gerards, M.; van den Bosch, B.; Calis, C.; Schoonderwoerd, K.; van Engelen, K.; Tijssen, M.; de Coo, R.; van der Kooi, A.; Smeets, H. Nonsense mutations in CABC1/ADCK3 cause progressive cerebellar ataxia and atrophy. *Mitochondrion* **2010**, *10*, 510-515, doi:10.1016/j.mito.2010.05.008.
22. Horvath, R.; Czermin, B.; Gulati, S.; Demuth, S.; Houge, G.; Pyle, A.; Dineiger, C.; Blakely, E.L.; Hassani, A.; Foley, C., et al. Adult-onset cerebellar ataxia due to mutations in CABC1/ADCK3. *Journal of neurology, neurosurgery, and psychiatry* **2012**, *83*, 174-178, doi:10.1136/jnnp-2011-301258.
23. Lagier-Tourenne, C.; Tazir, M.; Lopez, L.C.; Quinzii, C.M.; Assoum, M.; Drouot, N.; Busso, C.; Makri, S.; Ali-Pacha, L.; Benhassine, T., et al. ADCK3, an ancestral kinase, is mutated in a form of recessive ataxia associated with coenzyme Q10 deficiency. *Am J Hum Genet* **2008**, *82*, 661-672, doi:S0002-9297(08)00152-3 [pii] 10.1016/j.ajhg.2007.12.024.
24. Liu, Y.T.; Hersheson, J.; Plagnol, V.; Fawcett, K.; Duberley, K.E.; Preza, E.; Hargreaves, I.P.; Chalasani, A.; Laura, M.; Wood, N.W., et al. Autosomal-recessive cerebellar ataxia caused by a novel ADCK3 mutation that elongates the protein: clinical, genetic and biochemical characterisation. *Journal of neurology, neurosurgery, and psychiatry* **2014**, *85*, 493-498, doi:10.1136/jnnp-2013-306483.
25. Mignot, C.; Apartis, E.; Durr, A.; Marques Lourenco, C.; Charles, P.; Devos, D.; Moreau, C.; de Lonlay, P.; Drouot, N.; Burglen, L., et al. Phenotypic variability in ARCA2 and identification of a core ataxic phenotype with slow progression. *Orphanet journal of rare diseases* **2013**, *8*, 173, doi:10.1186/1750-1172-8-173.
26. Mollet, J.; Delahodde, A.; Serre, V.; Chretien, D.; Schlemmer, D.; Lombes, A.; Boddaert, N.; Desguerre, I.; de Lonlay, P.; de Baulny, H.O., et al. CABC1 gene mutations cause ubiquinone deficiency with cerebellar ataxia and seizures. *Am J Hum Genet* **2008**, *82*, 623-630, doi:10.1016/j.ajhg.2007.12.022.
27. Ashraf, S.; Gee, H.Y.; Woerner, S.; Xie, L.X.; Vega-Warner, V.; Lovric, S.; Fang, H.; Song, X.; Cattran, D.C.; Avila-Casado, C., et al. ADCK4 mutations promote steroid-resistant nephrotic syndrome through CoQ10 biosynthesis disruption. *J Clin Invest* **2013**, *123*, 5179-5189, doi:10.1172/JCI69000.
28. Simpson, K.J.; Selfors, L.M.; Bui, J.; Reynolds, A.; Leake, D.; Khvorova, A.; Brugge, J.S. Identification of genes that regulate epithelial cell migration using an siRNA screening approach. *Nature cell biology* **2008**, *10*, 1027-1038, doi:10.1038/ncb1762.
29. Wiedemeyer, W.R.; Dunn, I.F.; Quayle, S.N.; Zhang, J.; Chheda, M.G.; Dunn, G.P.; Zhuang, L.; Rosenbluh, J.; Chen, S.; Xiao, Y., et al. Pattern of retinoblastoma pathway inactivation dictates response to CDK4/6 inhibition in GBM. *Proc Natl Acad Sci U S A* **2010**, *107*, 11501-11506, doi:10.1073/pnas.1001613107.
30. Brough, R.; Frankum, J.R.; Sims, D.; Mackay, A.; Mendes-Pereira, A.M.; Bajrami, I.; Costa-Cabral, S.; Rafiq, R.; Ahmad, A.S.; Cerone, M.A., et al. Functional viability profiles of breast cancer. *Cancer discovery* **2011**, *1*, 260-273, doi:10.1158/2159-8290.CD-11-0107.
31. Schoolmeesters, A.; Brown, D.D.; Fedorov, Y. Kinome-wide functional genomics screen reveals a novel mechanism of TNFalpha-induced nuclear accumulation of the HIF-1alpha transcription factor in cancer cells. *PLoS One* **2012**, *7*, e31270, doi:10.1371/journal.pone.0031270.
32. Hughes, B.G.; Harrison, P.M.; Hekimi, S. Estimating the occurrence of primary ubiquinone deficiency by analysis of large-scale sequencing data. *Sci Rep* **2017**, *7*, 17744, doi:10.1038/s41598-017-17564-y.
33. Alcazar-Fabra, M.; Trevisson, E.; Brea-Calvo, G. Clinical syndromes associated with Coenzyme Q10 deficiency. *Essays in biochemistry* **2018**, *62*, 377-398, doi:10.1042/EBC20170107.

34. Qiu, L.Q.; Lai, W.S.; Stumpo, D.J.; Blackshear, P.J. Mouse Embryonic Fibroblast Cell Culture and Stimulation. *Bio Protoc* **2016**, *6*, doi:10.21769/BioProtoc.1859.
35. Richardson, A.; Fischer, K.E.; Speakman, J.R.; de Cabo, R.; Mitchell, S.J.; Peterson, C.A.; Rabinovitch, P.; Chiao, Y.A.; Taffet, G.; Miller, R.A., et al. Measures of Healthspan as Indices of Aging in Mice-A Recommendation. *J Gerontol A Biol Sci Med Sci* **2016**, *71*, 427-430, doi:10.1093/gerona/glv080.
36. Aartsma-Rus, A.; van Putten, M. Assessing functional performance in the mdx mouse model. *J Vis Exp* **2014**, *85*, e51303, doi:10.3791/51303.
37. Calvino-Nunez, C.; Dominguez-del-Toro, E. Clonidine treatment delays postnatal motor development and blocks short-term memory in young mice. *PLoS One* **2014**, *9*, e114869, doi:10.1371/journal.pone.0114869.
38. Dornelles, A.; de Lima, M.N.; Grazziotin, M.; Presti-Torres, J.; Garcia, V.A.; Scalco, F.S.; Roesler, R.; Schroder, N. Adrenergic enhancement of consolidation of object recognition memory. *Neurobiol Learn Mem* **2007**, *88*, 137-142, doi:10.1016/j.nlm.2007.01.005.
39. Rodriguez-Aguilera, J.C.; Cortes, A.B.; Fernandez-Ayala, D.J.; Navas, P. Biochemical Assessment of Coenzyme Q10 Deficiency. *J Clin Med* **2017**, *6*, doi:10.3390/jcm6030027.
40. Bentinger, M.; Tekle, M.; Brismar, K.; Chojnacki, T.; Swiezewska, E.; Dallner, G. Polyisoprenoid epoxides stimulate the biosynthesis of coenzyme Q and inhibit cholesterol synthesis. *J Biol Chem* **2008**, *283*, 14645-14653, doi:10.1074/jbc.M710202200.
41. Spinazzi, M.; Casarin, A.; Pertegato, V.; Salviati, L.; Angelini, C. Assessment of mitochondrial respiratory chain enzymatic activities on tissues and cultured cells. *Nature protocols* **2012**, *7*, 1235-1246, doi:10.1038/nprot.2012.058.
42. Salabei, J.K.; Gibb, A.A.; Hill, B.G. Comprehensive measurement of respiratory activity in permeabilized cells using extracellular flux analysis. *Nature protocols* **2014**, *9*, 421-438, doi:10.1038/nprot.2014.018.
43. Mitchell, S.J.; Madrigal-Matute, J.; Scheibye-Knudsen, M.; Fang, E.; Aon, M.; Gonzalez-Reyes, J.A.; Cortassa, S.; Kaushik, S.; Gonzalez-Freire, M.; Patel, B., et al. Effects of Sex, Strain, and Energy Intake on Hallmarks of Aging in Mice. *Cell Metab* **2016**, *23*, 1093-1112, doi:10.1016/j.cmet.2016.05.027.
44. Mitchell, S.J.; Bernier, M.; Aon, M.A.; Cortassa, S.; Kim, E.Y.; Fang, E.F.; Palacios, H.H.; Ali, A.; Navas-Enamorado, I.; Di Francesco, A., et al. Nicotinamide Improves Aspects of Healthspan, but Not Lifespan, in Mice. *Cell Metab* **2018**, *27*, 667-676 e664, doi:10.1016/j.cmet.2018.02.001.
45. Fernandez-Ayala, D.J.; Guerra, I.; Jimenez-Gancedo, S.; Cascajo, M.V.; Gavilan, A.; Dimauro, S.; Hirano, M.; Briones, P.; Artuch, R.; De Cabo, R., et al. Survival transcriptome in the coenzyme Q10 deficiency syndrome is acquired by epigenetic modifications: a modelling study for human coenzyme Q10 deficiencies. *BMJ open* **2013**, *3*, doi:10.1136/bmjopen-2012-002524.
46. Newman, J.C.; Verdin, E. beta-Hydroxybutyrate: A Signaling Metabolite. *Annu Rev Nutr* **2017**, *37*, 51-76, doi:10.1146/annurev-nutr-071816-064916.
47. Yu, Q.; Zhou, B.; Zhang, Y.; Nguyen, E.T.; Du, J.; Glosson, N.L.; Kaplan, M.H. DNA methyltransferase 3a limits the expression of interleukin-13 in T helper 2 cells and allergic airway inflammation. *Proc Natl Acad Sci U S A* **2012**, *109*, 541-546, doi:10.1073/pnas.1103803109.
48. Murphy, M.P.; O'Neill, L.A.J. Krebs Cycle Reimagined: The Emerging Roles of Succinate and Itaconate as Signal Transducers. *Cell* **2018**, *174*, 780-784, doi:10.1016/j.cell.2018.07.030.
49. Teveroni, E.; Pellegrino, M.; Sacconi, S.; Calandra, P.; Cascino, I.; Farioli-Vecchioli, S.; Puma, A.; Garibaldi, M.; Morosetti, R.; Tasca, G., et al. Estrogens enhance myoblast differentiation in facioscapulohumeral muscular dystrophy by antagonizing DUX4 activity. *J Clin Invest* **2017**, *127*, 1531-1545, doi:10.1172/JCI89401.
50. Horvath, R.; Schneiderat, P.; Schoser, B.G.; Gempel, K.; Neuen-Jacob, E.; Ploger, H.; Muller-Hocker, J.; Pongratz, D.E.; Naini, A.; DiMauro, S., et al. Coenzyme Q10 deficiency and isolated myopathy. *Neurology* **2006**, *66*, 253-255, doi:10.1212/01.wnl.0000194241.35115.7c.
51. Lalani, S.R.; Vladutiu, G.D.; Plunkett, K.; Lotze, T.E.; Adesina, A.M.; Scaglia, F. Isolated mitochondrial myopathy associated with muscle coenzyme Q10 deficiency. *Archives of neurology* **2005**, *62*, 317-320, doi:10.1001/archneur.62.2.317.
52. Stefely, J.A.; Pagliarini, D.J. Biochemistry of Mitochondrial Coenzyme Q Biosynthesis. *Trends Biochem Sci* **2017**, *42*, 824-843, doi:10.1016/j.tibs.2017.06.008.
53. Parrado-Fernandez, C.; Lopez-Lluch, G.; Rodriguez-Bies, E.; Santa-Cruz, S.; Navas, P.; Ramsey, J.J.; Villalba, J.M. Calorie restriction modifies ubiquinone and COQ transcript levels in mouse tissues. *Free Radic Biol Med* **2011**, *50*, 1728-1736, doi:10.1016/j.freeradbiomed.2011.03.024.

54. Yubero, D.; Montero, R.; Martin, M.A.; Montoya, J.; Ribes, A.; Grazina, M.; Trevisson, E.; Rodriguez-Aguilera, J.C.; Hargreaves, I.P.; Salviati, L., et al. Secondary coenzyme Q10 deficiencies in oxidative phosphorylation (OXPHOS) and non-OXPHOS disorders. *Mitochondrion* **2016**, *30*, 51-58, doi:10.1016/j.mito.2016.06.007.
55. Hernandez-Alvarez, M.I.; Sebastian, D.; Vives, S.; Ivanova, S.; Bartoccioni, P.; Kakimoto, P.; Plana, N.; Veiga, S.R.; Hernandez, V.; Vasconcelos, N., et al. Deficient Endoplasmic Reticulum-Mitochondrial Phosphatidylserine Transfer Causes Liver Disease. *Cell* **2019**, *177*, 881-895 e817, doi:10.1016/j.cell.2019.04.010.
56. Eisenberg-Bord, M.; Tsui, H.S.; Antunes, D.; Fernandez-Del-Rio, L.; Bradley, M.C.; Dunn, C.D.; Nguyen, T.P.T.; Rapaport, D.; Clarke, C.F.; Schuldiner, M. The Endoplasmic Reticulum-Mitochondria Encounter Structure Complex Coordinates Coenzyme Q Biosynthesis. *Contact (Thousand Oaks)* **2019**, *2*, 2515256418825409, doi:10.1177/2515256418825409.
57. Rinaldo, P.; Matern, D.; Bennett, M.J. Fatty acid oxidation disorders. *Annu Rev Physiol* **2002**, *64*, 477-502, doi:10.1146/annurev.physiol.64.082201.154705.
58. Schatz, U.A.; Ensenauer, R. The clinical manifestation of MCAD deficiency: challenges towards adulthood in the screened population. *Journal of inherited metabolic disease* **2010**, *33*, 513-520, doi:10.1007/s10545-010-9115-5.
59. Wicks, S.E.; Vandanmagsar, B.; Haynie, K.R.; Fuller, S.E.; Warfel, J.D.; Stephens, J.M.; Wang, M.; Han, X.; Zhang, J.; Noland, R.C., et al. Impaired mitochondrial fat oxidation induces adaptive remodeling of muscle metabolism. *Proc Natl Acad Sci U S A* **2015**, *112*, E3300-3309, doi:10.1073/pnas.1418560112.
60. Zhao, L.; Pascual, F.; Bacudio, L.; Suchanek, A.L.; Young, P.A.; Li, L.O.; Martin, S.A.; Camporez, J.P.; Perry, R.J.; Shulman, G.I., et al. Defective fatty acid oxidation in mice with muscle-specific acyl-CoA synthetase 1 deficiency increases amino acid use and impairs muscle function. *J Biol Chem* **2019**, *294*, 8819-8833, doi:10.1074/jbc.RA118.006790.
61. Ghosh, S.; Wicks, S.E.; Vandanmagsar, B.; Mendoza, T.M.; Bayless, D.S.; Salbaum, J.M.; Dearth, S.P.; Campagna, S.R.; Mynatt, R.L.; Noland, R.C. Extensive metabolic remodeling after limiting mitochondrial lipid burden is consistent with an improved metabolic health profile. *J Biol Chem* **2019**, 10.1074/jbc.RA118.006074, doi:10.1074/jbc.RA118.006074.
62. Li, L.O.; Grevengoed, T.J.; Paul, D.S.; Ilkayeva, O.; Koves, T.R.; Pascual, F.; Newgard, C.B.; Muoio, D.M.; Coleman, R.A. Compartmentalized acyl-CoA metabolism in skeletal muscle regulates systemic glucose homeostasis. *Diabetes* **2015**, *64*, 23-35, doi:10.2337/db13-1070.
63. Kozawa, S.; Honda, A.; Kajiwara, N.; Takemoto, Y.; Nagase, T.; Nikami, H.; Okano, Y.; Nakashima, S.; Shimozawa, N. Induction of peroxisomal lipid metabolism in mice fed a high-fat diet. *Molecular medicine reports* **2011**, *4*, 1157-1162, doi:10.3892/mmr.2011.560.
64. Schuster, S.; Cabrera, D.; Arrese, M.; Feldstein, A.E. Triggering and resolution of inflammation in NASH. *Nat Rev Gastroenterol Hepatol* **2018**, *15*, 349-364, doi:10.1038/s41575-018-0009-6.